Journal of Statistical Physics, Vol. 75, Nos. 3/4, 1994

Statistical Mechanics of Random Paths on Disordered Lattices

Achille Giacometti,[1,2] Amos Maritan,[3] and Hisao Nakanishi[1]

Received August 11, 1993; final February 1, 1994

The dependence of the universality class on the statistical weight of unrestricted random paths is explicitly shown both for deterministic and statistical fractals such as the incipient infinite percolation cluster. Equally weighted paths (ideal chain) and kinetically generated paths (random walks) belong, in general, to different universality classes. For deterministic fractals exact renormalization group techniques are used. Asymptotic behaviors for the end-to-end distance ranging from power to logarithmic (localization) laws are observed for the ideal chain. In all these cases, random walks in the presence of nonperfect traps are shown to be in the same universality class of the ideal chain. Logarithmic behavior is reflected in *singular* renormalization group recursions. For the disordered case, numerical transfer matrix techniques are exploited on percolation clusters in two and three dimensions. The two-point correlation function scales with critical exponents not obeying standard scaling relations. The distribution of the number of chains and the number of chains returning to the starting point are found to be well approximated by a log-normal distribution. The log-moment of the number of chains is found to have an essential type of singularity consistent with the log-normal distribution. A non-self-averaging behavior is argued to occur on the basis of the results.

KEY WORDS: Disordered systems; random walks; ideal polymers; fractals; percolation clusters; renormalization group.

1. INTRODUCTION

Stochastic processes have a very wide field of applications, ranging from biology to economics.[1] In physics the interest is also broad, from solid-state physics[1] to high-energy theory[2] to the physics of polymers.[3,4]

[1] Department of Physics, Purdue University, West Lafayette, Indiana 47907.
[2] Present address: Istituto di Fisica "Galileo Galilei," Padova, Italy.
[3] Dipartimento di Fisica, Università di Padova, and Istituto Nazionale di Fisica Nucleare Sezione di Padova, Padova, Italy, and Department of Physics, Pennsylvania State University, University Park, Pennsylvania 16802.

0022-4715/94/0500-0669$07.00/0

The problem of diffusion in disordered media is one of the most interesting for practical applications. Due to its complexity, only simple models have been investigated both analytically and numerically.[5] These models of random walks, however, have been for many years paradigm enabling us to grasp many of the essential features of the physics involved.

Very recently[7-9] it has been pointed out that the critical properties of the ideal chain are different from the random walk whenever the environment is not translationally invariant.

An ideal chain (IC) is a simple model for a polymer in solution in situations when the excluded-volume effect is negligible. It is of great theoretical interest also because it is known that the self-avoidance does not play any role above the critical dimension and because of its mapping with the model of the random walk in the presence of random (perfect) traps, which mimics, e.g., the physics of magnetic and optical excitations in the presence of defects.[10] A further reason to study this model is the lack of understanding of the case in the presence of excluded volume.[11]

In an IC a walk is generated on a lattice by giving equal weight to the steps independently of the coordination number of the particular site. In the literature (see, e.g., ref. 6) two other models of a random walk (RW) on a disordered lattice are commonly discussed: the *blind ant*, where the walker tries to jump to one of the nearest-neighbor sites with equal probability, but if one of the sites is not available, the ant remains in the present position; and the *myopic ant*, which instead always jumps with probability corresponding to the inverse of the local coordination number. The ideal chain can be thought of as the case of a blind ant which dies whenever it tries to jump into a nonavailable site, provided that the statistics is taken only for the surviving walks (see Section 2).

Despite their differences, the blind and myopic ants have been shown[12] to give equivalent asymptotic behavior for the net displacement in any lattice. This is not the case, however, for the IC. The main difference, besides the difference in the statistical weights given to each random path, is clearly that the IC is not a growth process (which never dies). This is also reflected in the spectral properties of the transition matrix.[4]

It is worthwhile to mention that we will study the situation where a walk can live only on the incipient infinite cluster, which is different from the case when such a restriction does not occur. The latter has been studied in the literature using (mainly but not only) field-theoretic techniques,[15] which, however, cannot be applied to the present problem. Also the simpler case when the walk is directed has been considered.[16]

On fully occupied (hyper)cubic lattices, where all the sites are available

[4] For the random walk see ref. 13; for the ideal chain see ref. 14.

and have the same coordination number, the ideal chain and both the ants clearly coincide. The same happens, apart from a trivial rescaling of time, for a periodic lattice with nonuniform coordination numbers (see Appendix C).

The first example where the ants and IC show different behavior is a deterministic self-similar structure (exact fractal), where the coordination numbers can be a (finite) integer set (see, e.g., ref. 17). A previous analysis[7] on some such structures showed that the critical exponents of the end-to-end distance and the susceptibility are different for the cases of the IC and the RW. The IC behavior of the end-to-end distance, however, was found to be strongly dependent on the particular structure of the lattice. When the sites with highest coordination formed an infinitely connected path, the exponent ν_c of the end-to-end distance $R_N \sim N^{\nu_c}$ was larger than the counterpart ν_w of the RW. However, when this was not the case, a slower diffusion, such as $R \sim \exp[(\log N)^{1/2}]$ or $R \sim (\log N)^{\psi}$ $(\psi > 0)$ was found.

A second example is a statistical fractal such as the percolation cluster on a square or cubic lattice at the percolation threshold, where we have shown[8] that the critical exponents are different for the IC and RW. Indeed we find a very pathological type of diffusion for the IC on each single configuration, taking place in the form of extended tails between regions in which the chain spends a lot of time. After a quenched average, however, a usual power law is recovered, but with a value $\nu > 1/2$ for the exponent of the end-to-end distance (superdiffusion), which is rather surprising. The distribution of the end-to-end distance is found to have a stretched-exponential form for large values of the argument, with an exponent δ not compatible with a scaling relation $\delta = (1-\nu)^{-1}$, which holds for the self-avoiding walk on a fully occupied lattice,[18] and was conjectured to hold true also for random walks on disordered lattices.[19]

The entropic behavior is also investigated. In the deterministic cases the susceptibility $\chi \sim (k_c - k)^{-\gamma}$ is found (where k is the variable conjugate to N) for the ideal chain to range from a value $\gamma_c = 1$ (which is the value for the random walk on any lattice, due to the conservation of the probability) to a different value. In the statistical fractal, on the other hand, the situation is quite different. The distribution of the number of N-step chains starting from the same point $\mathbf{x}_0$, $C_{\mathbf{x}_0}(N)$, is found to have a log-normal distribution whose variance grows faster than the mean value (which we call weak non-self-averaging). This feature is particularly important in relationship to the moments of the distribution, as will be discussed.

The aim of the present work is to recall some previous results[7-9] in a unified framework, and to present some new relevant results on the same subject.

The paper is organized as follows. After a definition of the general model in Section 2, the renormalization group (RG) approach to the deter-

ministic fractals is reviewed in Section 3. Then the numerical work on a statistical fractal (square and simple cubic lattice at the percolation threshold) is carried out, and the physical meaning of the results is discussed in Section 4. Section 5 is dedicated to the conclusions, and some technical details are given in the appendices.

2. RANDOM PATHS AND MAPPING INTO A GAUSSIAN MODEL

We will begin by recalling the simplest case of the random walk (RW) and of the ideal chain (IC) on a hypercubic lattice and after that generalizations to generic structures will be considered.

2.1. Ordered Lattice

A d-dimensional (hyper)cubic lattice with lattice spacing equal to 1 is defined by an orthonormal basis $\{\hat{\mathbf{e}}_\mu\}$ such that $\hat{\mathbf{e}}_\mu \cdot \hat{\mathbf{e}}_\nu = \delta_{\mu,\nu}$, $\mu, \nu = 1,..., d$. Then a lattice point $\mathbf{x} \in \mathbb{Z}^d$ will be indentified by a sequence of integers $\{x_\mu\}_{\mu=1,...,d}$. The master equation describing a RW is

$$P_{\mathbf{x}_0,\mathbf{x}}(N+1) = \frac{1}{z} \sum_{\mathbf{y}(\mathbf{x})} P_{\mathbf{x}_0,\mathbf{y}}(N) \tag{2.1}$$

where $P_{\mathbf{x}_0,\mathbf{x}}(N)$ is the probability of finding a walker at position $\mathbf{x}$ after N steps, given that it started at $\mathbf{x}_0$, and $z = 2d$ is the coordination number of the lattice. The notation $\mathbf{y}(\mathbf{x})$ means that the sum is restricted to the nearest neighbors of $\mathbf{x}$.

A standard procedure to solve Eq. (2.1) is to introduce the generating function (discrete Laplace transform)

$$G_{\mathbf{x}_0,\mathbf{x}}(\omega) = \sum_{N=0}^{+\infty} \frac{1}{z(1+\omega)^{N+1}} P_{\mathbf{x}_0,\mathbf{x}}(N) \tag{2.2}$$

where the factor $1/z$ has been introduced for future convenience. Then (2.1) and the initial condition $P_{\mathbf{x}_0,\mathbf{x}}(0) = \delta_{\mathbf{x}_0,\mathbf{x}}$ yields

$$\alpha_{\mathbf{x}} G_{\mathbf{x}_0,\mathbf{x}}(\omega) = \sum_{\mathbf{y}(\mathbf{x})} G_{\mathbf{x}_0,\mathbf{y}}(\omega) + \delta_{\mathbf{x}_0,\mathbf{x}} \tag{2.3}$$

where $\alpha_{\mathbf{x}} = z(1+\omega)$.

Similarly, the IC is defined through the number of N step chains $C_{\mathbf{x}_0,\mathbf{x}}(N)$ with extrema at $\mathbf{x}_0$ and $\mathbf{x}$, which obeys the recursion equation

$$C_{\mathbf{x}_0,\mathbf{x}}(N+1) = \sum_{\mathbf{y}(\mathbf{x})} C_{\mathbf{x}_0,\mathbf{y}}(N) \tag{2.4}$$

with initial condition $C_{\mathbf{x}_0,\mathbf{x}}(N=0)=\delta_{\mathbf{x}_0,\mathbf{x}}$. The generating function for $C_{\mathbf{x}_0,\mathbf{x}}(N)$, analogous to (2.2),

$$\tilde{G}_{\mathbf{x}_0,\mathbf{x}}(k)=\sum_{N=0}^{+\infty} k^N C_{\mathbf{x}_0,\mathbf{x}}(N)=\sum_{w:\partial w=\{\mathbf{x}_0,\mathbf{x}\}} k^{|w|} \tag{2.5}$$

where $|w|$ is the number of steps associated with the walk w and ∂w is its boundary, satisfies an equation of the form (2.3) with $\alpha_{\mathbf{x}}=1/k$. This implies that the two problems are equivalent to each other with the correspondence

$$P_{\mathbf{x}_0,\mathbf{x}}(N)=\frac{C_{\mathbf{x}_0,\mathbf{x}}(N)}{z^N} \tag{2.6a}$$

$$k=\frac{1}{z(1+\omega)} \tag{2.6b}$$

$$k\tilde{G}_{\mathbf{x}_0,\mathbf{x}}(k)=G_{\mathbf{x}_0,\mathbf{x}}(\omega) \tag{2.6c}$$

Clearly k has the interpretation of a fugacity per step for the IC where the trajectories are all equally weighted. Criticality is reached in the limit $\omega\to 0^+$, i.e., $k\to k_c^-$, $k_c=1/z$. When $k>k_c$ then $\tilde{G}_{\mathbf{x}_0,\mathbf{x}}$ is infinite.

A very convenient way of treating both models is to consider a Gaussian model for a scalar free-field theory with the Hamiltonian

$$H(\{\phi\})=\tfrac{1}{2}\sum_{\mathbf{x},\mathbf{y}} \phi_{\mathbf{x}}(1-K)_{\mathbf{x},\mathbf{y}}\phi_{\mathbf{y}} \tag{2.7}$$

where

$$(K)_{\mathbf{x},\mathbf{y}}=\begin{cases} k & \text{if } |\mathbf{x}-\mathbf{y}|=1 \\ 0 & \text{otherwise} \end{cases} \tag{2.8}$$

is the standard hopping matrix.

The partition function is then

$$\begin{aligned} Z(\{h\}) &= \int \mathscr{D}\phi \exp\left[-H(\{\phi\})+\sum_{\mathbf{x}} h_{\mathbf{x}}\phi_{\mathbf{x}}\right] \\ &= [\det(1-K)]^{-1/2}\exp\left[\tfrac{1}{2}\sum_{\mathbf{x},\mathbf{y}} h_{\mathbf{x}}(1-K)^{-1}_{\mathbf{x},\mathbf{y}}h_{\mathbf{y}}\right] \end{aligned} \tag{2.9}$$

where $\mathscr{D}\phi=\prod_{\mathbf{x}} d\phi_{\mathbf{x}}/(2\pi)^{1/2}$ and $h_{\mathbf{x}}$ are the external fields introduced to calculate the various correlation functions by deriving Eq. (2.9) with respect to the h's.

Then it is immediate to see that the two-point correlation function

$$\langle \phi_{\mathbf{x}_0} \phi_{\mathbf{x}} \rangle = \left. \frac{\partial^2 \log Z}{\partial h_{\mathbf{x}} \, \partial h_{y}} \right|_{h=0} = (1-K)^{-1}_{\mathbf{x}_0, \mathbf{x}} \tag{2.10}$$

coincides with $\tilde{G}_{\mathbf{x}_0, \mathbf{x}}(k)$ defined in Eq. (2.5). Indeed Eq. (2.10) can be explicitly evaluated by means of a von Neumann expansion:

$$\begin{aligned} \langle \phi_{\mathbf{x}_0} \phi_{\mathbf{x}} \rangle &= \sum_{N=0}^{+\infty} (K^N)_{\mathbf{x}_0, \mathbf{x}} \\ &= \sum_{N=0}^{+\infty} k^N \sum_{\{\mathbf{x}_1, \ldots, \mathbf{x}_{N-1}\}} \prod_{N'=0}^{N-1} \delta_{1, |\mathbf{x}_{N'+1} - \mathbf{x}_{N'}|} \\ &= \sum_{N=0}^{+\infty} C_{\mathbf{x}_0, \mathbf{x}}(N) \, k^N \end{aligned} \tag{2.11}$$

which coincides with Eq. (2.5). Note that for $k > k_c$ the kernel $1-K$ is no longer positive definite.

The generating function χ for all walls with a fixed extremum is given by

$$\chi(k) = \sum_{\mathbf{x}} \tilde{G}_{\mathbf{x}_0, \mathbf{x}}(k) = (1 - zk)^{-1} = z^{-1}(k_c - k)^{-\gamma} \tag{2.12}$$

where $\gamma = 1$. χ plays a role similar to the susceptibility for magnetic systems.[3,4]

To conclude this simple case, we recall the relation between the canonical ensemble (defined by N) and the grand-canonical ensemble (defined by the fugacity k).

The average number of steps for a walk w is given by

$$\langle |w| \rangle = \frac{\sum_w |w| \, k^{|w|}}{\sum_w k^{|w|}} = k \frac{\partial}{\partial k} \log \chi(k) \overset{k \to k_c}{\sim} \frac{\gamma k_c}{k_c - k} \tag{2.13}$$

One can thus pass from the canonical critical limit ($N \to \infty$) to the grand-canonical limit ($k \to k_c$) with the replacement

$$N \to \begin{cases} (k_c - k)^{-1} & \text{for IC} \\ \omega^{-1} & \text{for RW} \end{cases} \tag{2.14}$$

2.2. Disordered Lattice

Let us now consider the more complex case of a disordered lattice where the walks or chains are allowed to move only on a certain subset of occupied sites of an otherwise order lattice.

The general master equation for a random walk with nearest-neighbor hopping is

$$P_{\mathbf{x}_0,\mathbf{x}}(N+1) = P_{\mathbf{x}_0,\mathbf{x}}(N) + \sum_{\mathbf{y}(\mathbf{x})} [w_{\mathbf{x},\mathbf{y}} P_{\mathbf{x}_0,\mathbf{y}}(N) - w_{\mathbf{y},\mathbf{x}} P_{\mathbf{x}_0,\mathbf{x}}(N)] \quad (2.15)$$

where $w_{\mathbf{x},\mathbf{y}}$ is the probability to jump from $\mathbf{y}$ to $\mathbf{x}$ and it is different from zero only if $\mathbf{x}$ and $\mathbf{y}$ are occupied sites.

Two typical models are the *blind ant* $w_{\mathbf{x},\mathbf{y}} = 1/z$ and the *myopic ant* $w_{\mathbf{x},\mathbf{y}} = 1/z_{\mathbf{y}}$, where $z_{\mathbf{x}}$ is the number of the nearest neighbors of $\mathbf{x}$ and z is the full coordination number of the lattice.[6,7] The IC keeps the same form as before since each walk is equally weighted. The only difference from the case on the hypercubic lattice is that the sum in Eq. (2.4) is restricted only to the occupied sites. Figure 1 illustrates the difference of these three models in terms of the hopping probability.

The blind ant and the IC with the identification (2.6a) can be cast in the following compact form (*imperfect blind ant*):

$$P_{\mathbf{x}_0,\mathbf{x}}(N+1) = q \frac{(z - z_{\mathbf{x}})}{z} P_{\mathbf{x}_0,\mathbf{x}}(N) + \frac{1}{z} \sum_{\mathbf{y}(\mathbf{x})} P_{\mathbf{x}_0,\mathbf{y}}(N) \quad (2.16)$$

where $q = 0, 1$ for the ideal chain and the blind ant, respectively.

The parameter q [$\in (0, 1)$] has a clear physical meaning in terms of random walks. The imperfect blind ant has a probability q to survive and remain in the same position when it does not jump into one of the allowed sites. In the $q \neq 1$ case the averages are concerned only with the surviving ants, i.e., normalized weights $P_{\mathbf{x}_0,\mathbf{x}}(N)/\sum_{\mathbf{x}} P_{\mathbf{x}_0,\mathbf{x}}(N)$ will be used. Thus the IC corresponds to the limiting case where the *ant* dies when it jumps to an unoccupied sites, which plays the role of a perfect trap (see ref. 10 and reference therein).

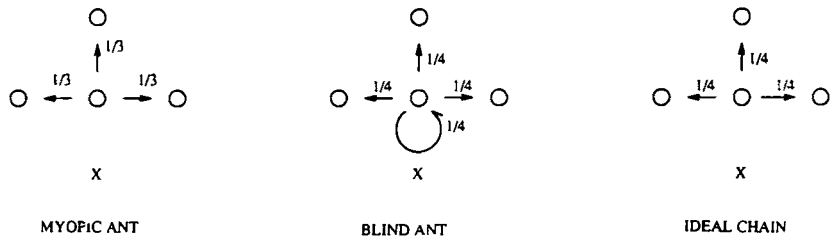

Fig. 1. Comparison of myopic ant, blind ant, and ideal chain in a situation where there are, in two dimensions, three sites available (○) and one not available (×).

Since in all the considered cases $w_{x,y} \equiv w_y$ depends only on y, defining the generating function

$$G_{x_0,x}(\omega) = w_x \sum_{N=0}^{+\infty} \frac{1}{(1+\omega)^{N+1}} P_{x_0,x}(N) \tag{2.17}$$

we find that Eq. (2.15) becomes

$$\alpha_x G_{x_0,x}(\omega) = \sum_{y(x)} G_{x_0,x}(\omega) + \delta_{x_0,x} \tag{2.18}$$

with

$$\alpha_x = \begin{cases} z_x(1+\omega) & \text{myopic ant} \\ z[\omega + z_x/z + (1-q)(1-z_x/z)] & \text{imperfect blind ant} \end{cases} \tag{2.19}$$

The IC case is obtained from Eq. (2.19) for $q=0$ and it gives again Eq. (2.6b) for the step fugacity.

The Gaussian model giving $G_{x_0,x} = \langle \phi_{x_0} \phi_x \rangle$ has the following Hamiltonian:

$$H(\{\phi\}), \{h\}) = \tfrac{1}{2} \sum_x \alpha_x \phi_x^2 - \sum_{\langle x,y \rangle} \phi_x \phi_y - \sum_x h_x \phi_x \tag{2.20}$$

and the sums are over occupied sites. This Hamiltonian is the same as in Eq. (2.7), upon a simple redefinition of the fields, and after we add a coupling with some external fields $\{h\}$'s in order to calculate the various correlation functions.

The conservation of probability holds, of course, only in the case of the myopic and blind ants, i.e.,

$$\sum_x P_{x_0,x}(N) = 1 \qquad (\forall N) \tag{2.21}$$

From Eqs. (2.21) and (2.17), one immediately has the *susceptibility*

$$\chi = \sum_x G_{x_0,x}(\omega) \sim \omega^{-1} \tag{2.22}$$

for the blind ant, implying that the *critical* value of ω is 0 (i.e., infinite-time limit). The same asymptotic behavior (2.22) holds also for the myopic ant: indeed, since $w_x = 1/z_x$ is bounded by $1/z$ from below and by 1 from above, one has

$$(z\omega)^{-1} \leqslant \sum_x z_x G_{x_0,x}(\omega) \leqslant \omega^{-1} \tag{2.23}$$

On the contrary, for the IC the critical value k_c of the step fugacity k is not known *a priori* and in general one assumes

$$\chi = \left\langle \sum_{\mathbf{x}} \tilde{G}_{\mathbf{x}_0,\mathbf{x}}(k) \right\rangle_0 \sim (k_c - k)^{-\gamma} \tag{2.24}$$

where γ is a critical exponent. In Eq. (2.24) the identification (2.6b), (2.6c) has been used and $\langle \cdot \rangle_0$ indicates the average over the starting points $\mathbf{x}_0$ [not necessary in Eq. (2.22)!]. If Eq. (2.24) holds, then from Eq. (2.5) it is easily verified that

$$\left\langle \sum_{\mathbf{x}} C_{\mathbf{x}_0,\mathbf{x}}(N) \right\rangle_0 \sim k_c^{-N} N^{\gamma - 1} \tag{2.25}$$

in the large-N limit (this follows from a Tauberian theorem[20]). Equations (2.22) and (2.24) also yield $\gamma = 1$ for random walks on any structure (disordered or not).

In Section 4.2 we will encounter a case in which the singularity is of an *essential* type, that is, we have, instead of (2.25),

$$\left\langle \sum_{\mathbf{x}} C_{\mathbf{x}_0,\mathbf{x}}(N) \right\rangle_0 \sim k_c^{-N} \exp(-aN^{\psi}) \tag{2.26}$$

with $0 < \psi < 1$ and $a > 0$. A saddle point approximation then gives

$$\operatorname{Im} \chi(k) \sim \exp(-|k_c - k|)^{-\psi/(1-\psi)} \tag{2.27}$$

for $k \to k_c$, which has the form of an essential singularity.[5]

The asymptotic behavior of the end-to-end distance is defined as

$$\langle R^2 \rangle = \frac{\sum_{\mathbf{x}_0,\mathbf{x}} G_{\mathbf{x}_0,\mathbf{x}}(\omega)(\mathbf{x} - \mathbf{x}_0)^2}{\sum_{\mathbf{x}_0,\mathbf{x}} G_{\mathbf{x}_0,\mathbf{x}}(\omega)} \tag{2.28a}$$

$$\sim \begin{cases} \omega^{-2\nu_w} & \text{for the ants (RW)} \\ (k_c - k)^{-2\nu_c} & \text{for the IC} \end{cases} \tag{2.28b}$$

which with the correspondence (2.14) can be rewritten in terms of the walk length N.

It is well known that for the hypercubic lattice[1] $k_c = 1/z$ and for any translationally invariant lattice $\nu_c = \nu_w = 1/2$ and $\gamma = 1$. For any lattice, disordered or not, both myopic and blind and have the same asymptotic behavior,[12] i.e., the same ν_w. This is the reason we used only one exponent

[5] Similar types of singularities were found for branched polymers in ref. 21.

in (2.28b) for the RW. It is evident that in a translationally invariant lattice where the coordination number z_x is a periodic function, the IC and the RW must have the same asymptotic behavior. This is discussed in Appendix C.

3. RENORMALIZATION GROUP FOR DETERMINISTIC CASE

Our aim is now to investigate the effect of a non-translationally-invariant lattice on the critical behavior for the models described in the previous section. We will start with some deterministic fractals where the breaking of the translational invariance of the lattice comes from the particular topology of the hierarchical structure considered, but which are nevertheless very handy for grasping the main features of interest. Some of the results of this section appeared in ref. 7.

3.1. The T-Fractal

The first example we will consider is the T-fractal. Figure 2 shows the first two steps T_1 and T_2 of the iterative construction of the lattice. Clearly its fractal dimension[17] is $\bar{d} = \log 3/\log 2$. This example is simple enough for a description of the general procedure, and contains some of the essential features of more complicated cases.

We start from the usual partition function

$$Z(\{h\}) = \int \mathscr{D}\phi \, e^{-H(\{\phi\},\{h\})} \tag{3.1}$$

where $H(\{\phi\}, \{h\})$ is the Hamiltonian defined in (2.20).

We can now pass from the stage T_n to the stage T_{n-1} by integrating on a suitable set of *fast variables* $\{\phi^f\}$,[22] so that

$$e^{-H'(\{\phi\},\{h'\})} = \text{const} \cdot \int \mathscr{D}\phi^f \, e^{-H(\{\phi^f,\phi^s\},\{h\})}\big|_{\phi=\zeta\phi^s} \tag{3.2}$$

where $\{\phi^s\}$ are the *slow variables* and ζ is the wave function renormalization which will be determined by fixing, e.g., to 1 the coefficient of the second sum in Eq. (2.20), i.e., the hopping term.

The overall result is that Z is unchanged. Since there are only two types of coordination, the RG procedure will involve only two parameters, i.e., $\alpha_x = \alpha_1, \alpha_3$ corresponding to $z_x = 1, 3$, respectively. Using the well-known result of the Gaussian integrals, namely

$$\int \mathscr{D}\phi \, e^{-\phi^T M\phi/2 + \phi^T J} = \frac{1}{(\det M)^{1/2}} e^{J^T M^{-1} J/2} \tag{3.3}$$

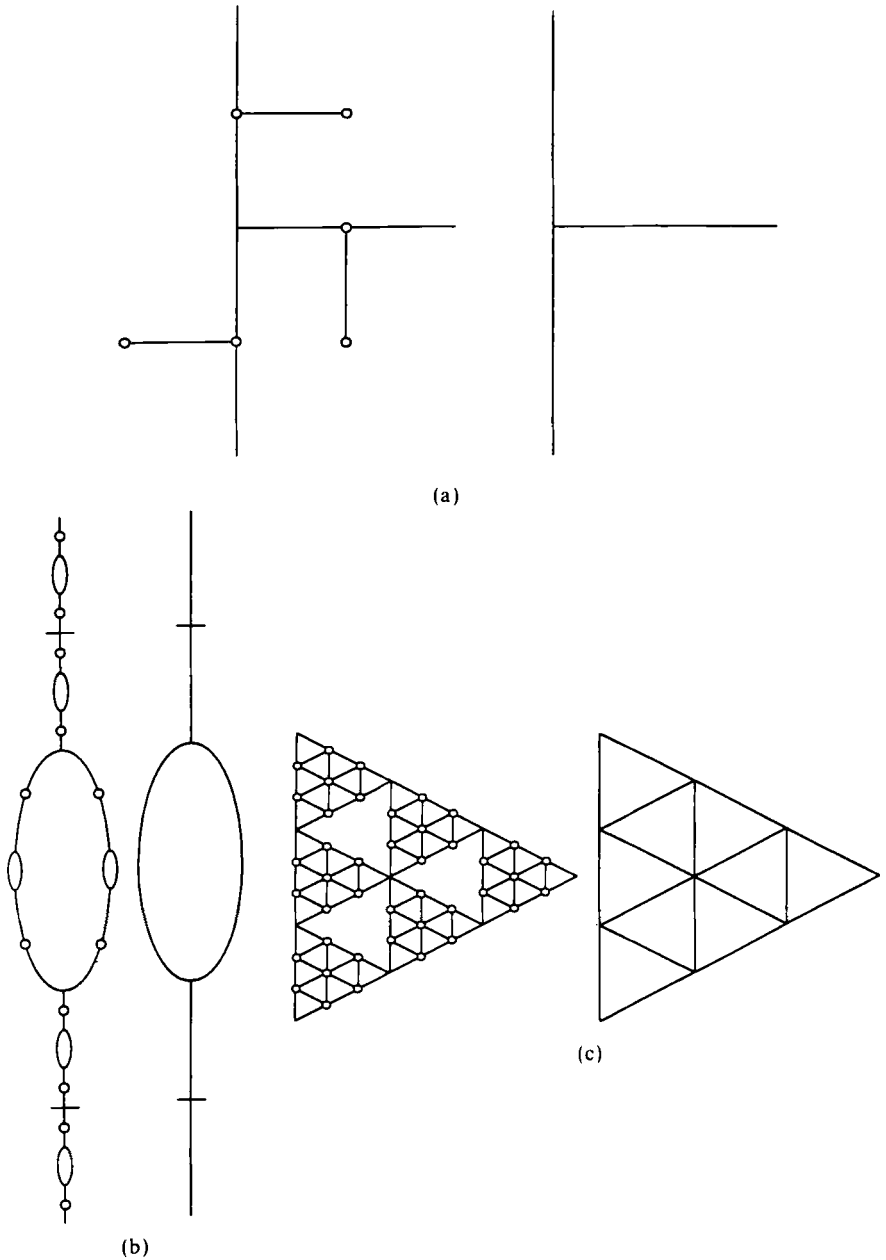

Fig. 2. Iterative construction of ((a) the T-fractal, (b) the blob-link model, and (c) the Sierpinski gasket with generator 3.

(the factor 2π has been absorbed in the definition of the measure) valid for any positive-definite real and symmetric matrix M, one can easily see that the minimal subset of variables acting as fast variables is identified by circles in Fig. 2. This will rescale the unit length by a factor 2. Equation (3.2) will then lead to the Hamiltonian H' of the same form as H with renormalized parameters $\alpha_x \equiv \alpha_{z_x}$ given by the recursion relations

$$\alpha_1' = \alpha_1 \alpha_3 - 2 \tag{3.4a}$$

$$\alpha_3' = \alpha_3^2 - \frac{\alpha_3}{\alpha_1} - 3 \tag{3.4b}$$

and *a wave function* renormalization

$$\zeta = \left(\frac{\alpha_1}{\alpha_1 \alpha_3 - 1} \right)^{1/2} \tag{3.5}$$

The coupling with the external fields $\{h\}$ leads also to two recursion relations for the two fields involved $h_x = h_1, h_3$ corresponding to sites of coordination 1 and 3, respectively:

$$h_1' = \frac{\alpha_1(\alpha_3 h_1 + h_3)}{[\alpha_1(\alpha_1 \alpha_3 - 1)]^{1/2}} \tag{3.6a}$$

$$h_3' = \frac{3h_1 + h_3(\alpha_3 \alpha_1 + 3\alpha_1 - 1)}{[\alpha_1(\alpha_1 \alpha_3 - 1)]^{1/2}} \tag{3.6b}$$

An analysis of the recursions (3.4a), (3.4b) will give information on the asymptotic behavior of the end-to-end distance,

$$\langle R_N^2 \rangle^{1/2} \overset{N \gg 1}{\sim} N^{1/d_i} \tag{3.7}$$

where $d_i = 1/\nu_i$ is the fractal dimension of the walk ($i = w$) or the chain ($i = c$). Figure 3 shows the resulting phase diagram. There are two fixed points, $W = (\alpha_1^* = 1, \alpha_3^* = 3)$ and $C = (\alpha_1^* = +\infty, \alpha_3^* = (1 + \sqrt{13})/2$ corresponding to the walk and the chain, respectively. Indeed in the former case, from Eq. (2.19) one has that $\alpha_x \to z_x$ as $\omega \to 0$ (both for blind and myopic ants), i.e., the two initial condition lines b: $\alpha_3 = \alpha_1 + 2$ for the blind ant and m: $\alpha_3 = 3\alpha_1$ for the myopic ant meet at the point W. Notice that the line $\alpha_3 = 3\alpha_2$ is an invariant set under RG transformation (3.4a), (3.4b). In other words both the blind and the myopic ant are controlled by the same fixed point W, in agreement with a general result.[12] The matrix $(\partial \alpha_i'/\partial \alpha_j)$ at W has two eigenvalues $\lambda_w = 6, 2$, the largest of which gives the exponent

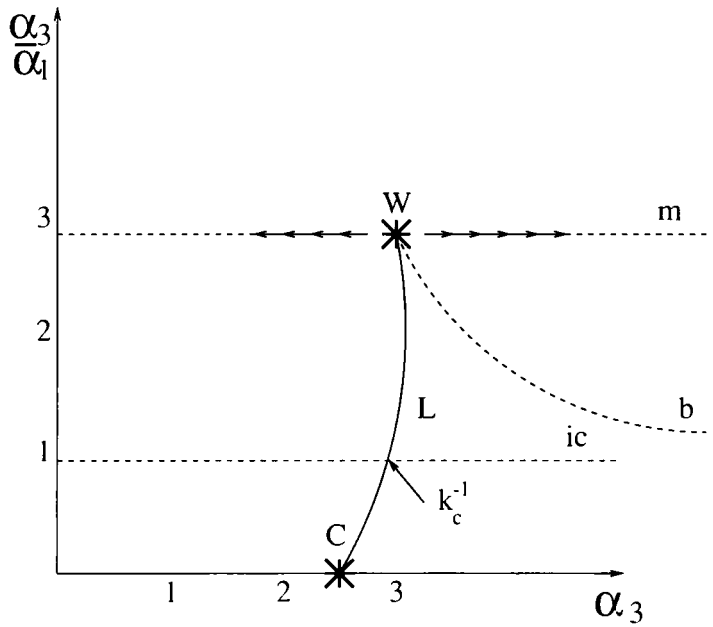

Fig. 3. Flow diagram for the case of the T-fractal: the fixed points W and C correspond to the random walk and ideal chain, respectively. The initial conditions m, b, and ic correspond to the myopic ant, the blind ant, and the ideal chain, respectively.

$d_w = \log \lambda_w / \log 2 = 2.585$ of the end-to end distrance defined in (3.7) as follows from standard renormalization group arguments.[22]

From the Alexander–Orbach relation[23] we can also evaluate the spectral dimension $\tilde{d}_w = 2\tilde{d}/d_w = 2 \log 3/\log 6$ describing the density of states, in the low-frequency limit, for the corresponding model of harmonic oscillators on the same structure. Using the parametrization $x = \alpha_3$ and $y = \alpha_3/\alpha_1$, we find that the recursion equations (3.4a), (3.4b) become

$$x' = x^2 - y - 3 \tag{3.8a}$$

$$y' = y \frac{x^2 - y - 3}{x^2 - 2y} \tag{3.8b}$$

from which the fixed point C, $(x^* = (1 + \sqrt{13})/2,\ y^* = 0)$, evident. Linearizing the above equations around C, one finds the two eigenvalues $\lambda = 1 - (3/x^{*2})$ and $2x^*$, corresponding to attractive and repulsive eigendirections, respectively. C describes the critical behavior of the ideal chain.

To show this, one can construct perturbatively around C a critical line L: $\alpha_3 = \alpha_3(\alpha_1)$ by imposing the constraint $\alpha_3' = \alpha_3(\alpha_1')$ [i.e., it is invariant under the map (3.4a), (3.4b)]. The first two terms are

$$\alpha_3 = x^* + \frac{x^{*2}}{(2x^{*2}-1)}\frac{1}{\alpha_1} + o\left(\frac{1}{\alpha_1^2}\right) \tag{3.9}$$

Then numerically one can see that this line originates from W and is attracted by C. The initial conditions line *ic* for the IC meets the critical line L when $k_c^{-1} = 2.536...$ and thus C controls its critical behavior. Indeed C controls the critical behavior of all initial conditions corresponding to the blind ant in the presence of imperfect traps [i.e., $0 \leqslant q < 1$ in Eq. (2.19)] since W does not have a domain of attraction. The exponent defined in (3.7) is thus $d_c = \log(2x^*)/\log 2 = 2.203...$, which is smaller than d_w, i.e., $\nu_c > \nu_w$! We further notice that the second relevant eigenvalue $\lambda_w = 2$ at W describes the crossover from RW to IC. We now turn to the calculation of the γ exponent, describing the critical behavior of the susceptibility

$$\chi(k) = \lim_{S\to\infty} \frac{1}{S}\sum_{\mathbf{x},\mathbf{y}} G_{\mathbf{x},\mathbf{y}}(k) \overset{k\to k_c}{\sim} (k_c - k)^{-\gamma} \tag{3.10}$$

where S is the number of sites of the T-fractal.

In this case we have to calculate the highest eigenvalue $\lambda_h = 2^{y_h}$ of the matrix associated with the linear mapping in Eqs. (3.6a), (3.6b) whose coefficients are calculated at the fixed point (α_1^*, α_3^*). The γ exponent is given by the standard relation[22,24]

$$\gamma_i = \frac{2y_h - \bar{d}}{d_i} \tag{3.11}$$

where $i = w, c$. At W, we get $\gamma_w = 1$, in agreement with the general argument given in the previous section, while at C,

$$\gamma_c = \frac{\log(5 + 2\sqrt{13})/3}{\log(1+\sqrt{13})} = 0.919...$$

It is also easy to compute the return probability (probability to return to the starting point $\mathbf{x}_0$ after N steps), which is equal to $P_{\mathbf{x}_0,\mathbf{x}_0}(N)$ appearing in the master equation only if conservation of probability holds. From the renormalization (3.5) one gets, in terms of the two-point correlation function,

$$G_{\mathbf{x}_0,\mathbf{x}_0}(\alpha_1, \alpha_2) = \frac{\alpha_1\alpha_3 - 1}{\alpha_1} G_{\mathbf{x}_0,\mathbf{x}_0}(\alpha_1', \alpha_3') \tag{3.12}$$

Close to the fixed point W, along the invariant line $\alpha_3 = 3\alpha_1 = 3(1+\omega)$, one has that $G_{\mathbf{x}_0,\mathbf{x}_0}(\alpha_1, \alpha_2) \equiv G_{\mathbf{x}_0,\mathbf{x}_0}(\omega)$, due to Eq. (3.12), obeys the scaling relation

$$G_{\mathbf{x}_0,\mathbf{x}_0}(\omega) = 2G_{\mathbf{x}_0,\mathbf{x}_0}(6\omega) \tag{3.13}$$

and thus

$$G_{\mathbf{x}_0,\mathbf{x}_0}(\omega) \overset{\omega \to 0}{\sim} \omega^{\tilde{d}_w/2-1} \tag{3.14}$$

where $\tilde{d}_w/2 = \log 3/\log 6 = \bar{d}/d_w$, in agreement with the Alexander–Orbach (AO) relation.[23] On the other hand, close to the other fixed point C, one finds

$$G_{\mathbf{x}_0,\mathbf{x}_0}(k) \overset{k \to k_c}{\sim} (k_c - k)^{\nu_c - 1} \tag{3.15}$$

In this case, however, the return probability is

$$P(\mathbf{0}, N) = \frac{C_{\mathbf{x}_0,\mathbf{x}_0}(N)}{\sum_{\mathbf{x}} C_{\mathbf{x}_0,\mathbf{x}}(N)} \tag{3.16}$$

due to the different normalization from the translationally invariant case. Since one expects that for large N

$$C_N \equiv \sum_{\mathbf{x}} C_{\mathbf{x}_0,\mathbf{x}}(N) \sim N^{\gamma-1} K_c^{-1} \tag{3.17}$$

then, using Eqs. (3.15), (3.17), we get for the exponent $\tilde{d}_c$ which *defines* the long-time behavior of the return probability that $\tilde{d}_c/2 = \nu_c + \gamma_c - 1$, which is *smaller* then the value expected from the AO relation. This is not a surprise, since $\tilde{d}_c$ does not bear the same physical meaning (as $\tilde{d}_w$) of spectral dimension for the low-frequency limit for the vibrational problem on the same structure. A similar mapping can, however, be implemented, leading, in the disordered case, to a Lifshits tail for the density of states of the transition matrix (see ref. 14).

We can now summarize what we have learned from this simple example.

(a) The problem of IC and RW are different when there is a non-translational-invariant environment, and they may belong to different universality classes (i.e., they have different critical exponents).

(b) The ideal chain is controlled by a fixed point where the fugacity corresponding to steps visiting sites with lowest coordination ($z_1 = 1$ in the T-fractal case) goes to zero. Indeed the corresponding parameter (α_1 in the present case) iterates to infinity after few recursions, while the other remains finite. We interpret this result by saying that the main contribution to the correlation function $G_{\mathbf{x}_0,\mathbf{x}}$ at the coarse-grained level comes from

chains which try to avoid sites at low coordination (z_1 in the present case.) Furthermore, the blind ant which dies with probability $(1-q)(z-z_{\mathbf{x}})/z$ ($q<1$) when visiting the site $\mathbf{x}$ has the same asymptotic behavior of the IC.

(c) Whenever, as in this case, the sites with highest coordination ($z_3=3$ in the present case) form an infinite connected cluster, then the IC goes further with respect to the RW, i.e., $\nu_c > \nu_w$.

3.2. The Blob-Link Model: Entropic Trapping

We now ask what happens if sites with highest coordination are forced to be not connected into an infinite cluster. The next example (the blob-link lattice) has exactly this feature (see Fig. 2). It was introduced[25] as deterministic model to mimic the behavior of the backbone incipient infinite cluster at the percolation threshold, and its fractal dimension is $\bar{d}=\log 6/\log l$, where l (>1) is some unspecified cale factor. Now there are still two types of coordinations, $z_{\mathbf{x}}=2, 3$, and therefore only two parameter, $\alpha_{\mathbf{x}}=\alpha_2$, α_3 and two external fields, $h_{\mathbf{x}}=h_2, h_3$, are needed. The minimal set of fast variables is indicated again by the open circles. This will scale the structure by a factor l.

The calculation for the recursion relation goes along the same line as the previous example. For the α's we get

$$\alpha_2' = \tfrac{1}{2}a_3^2\alpha_2(\alpha_2^2-2)+\alpha_3(1-\alpha_2^2)-2\alpha_2^3+\tfrac{9}{2}\alpha_2 \tag{3.18a}$$

$$\alpha_3' = \tfrac{1}{2}\alpha_3^2\alpha_2(\alpha_2\alpha_3-5)+2\alpha_3(1-\alpha_2^2)+6\alpha_2 \tag{3.18b}$$

There is an ordinary fixed point $W=(\alpha_2^*=2, \alpha_3^*=3)$, which obviously describes the behavior of the RW (both blind and myopic ant) as before. The asymptotic behavior of the end-to-end distance is like Eq. (3.7) with $d_w=\log 27/\log l$, which gives for the spectral dimension $\tilde{d}_w=2\bar{d}/d_w=2\log 6/\log 27=1.087\ldots$.

However, it appears that the point $C=(\alpha_2^*=+\infty, \alpha_3^*=+2)$ can be considered as a fixed point. Again there is a critical line L connecting W with C. As in the case of the T-fractal, C attracts the whole line L. The intersection of this line with the line of the initial condition c: $\alpha_2=\alpha_3=1/k$ occurs at $k_c^{-1}=2.63522\ldots$.

The first few terms around C of the critical line L, to be derived perturbatively around C in the same way as the previous example, are

$$\alpha_3(\alpha_2)=2+\frac{1}{\alpha_2}+\frac{5}{4}\frac{1}{\alpha_2^2}+o\left(\frac{1}{\alpha_2^3}\right) \tag{3.19}$$

Along this line, α_2 renormalized as

$$\alpha_2' = \frac{5}{2}\alpha_2 + \frac{7}{10} + o\left(\frac{1}{\alpha_2}\right) \tag{3.20}$$

We note, however, that C is not an ordinary fixed point as in the previous example, since it is infinitely repulsive. The standard method of linearizing the recursions around the fixed point then does not work. In Appendix A we describe a general method[7] to deal with such a case, and show that it reduces to the standard one whenever the linearization is possible.

Using the procedure described there, and in particular Eq. (A5) along with the critical line (3.19) and Eq. (3.20), one finds

$$\delta' = (2\alpha_2)^2 \delta + o(\alpha_2, \delta^2) \tag{3.21}$$

where δ is a measure of the distance from the critical line L and we take $\delta = k_c - k \ll 1$ initially.

By interating n times the leading order in Eq. (3.21), one finds, using (3.20),

$$\delta^{(n)} = (2\alpha_2)^{2n} \left[\prod_{p=0}^{n-1} (\tfrac{5}{2})^p\right]^2 \delta = \lambda_1^{n^2} \lambda_2^n \delta \tag{3.22}$$

where $\lambda_1 = 5/2$ and $\lambda_2 = (8\alpha_2^2/5)$. It is worth noticing that while the subleading term λ_2 depends on the initial conditions, since α_2 is one of the two coordinates of the starting point close to the critical line L, the leading term is universal.

Now we will consider the scaling of the correlation length $\xi(\alpha_2, \alpha_3) \equiv \langle R^2 \rangle^{1/2}$ for a starting point close to the critical line (3.19); after n recursions it becomes

$$\xi(\alpha_2, \alpha_3(\alpha_2) + \delta) = l^n \xi(\alpha_2^{(n)}, \alpha_3(\alpha_2^{(n)}) + \delta^{(n)}) \tag{3.23}$$

If we are close to criticality, then we can assume $\delta^{(n)} \equiv \bar{\delta} \ll 1$, and then (3.22) gives

$$n = \left[\frac{\log(\bar{\delta}/\delta)}{\log \lambda_1}\right]^{1/2} \tag{3.24}$$

where subleading terms have been dropped. Use of (3.24) in (3.23) then results in an expression for $\hat{\xi}(k) \equiv \xi(\alpha_2 = 1/k, \alpha_3 = 1/k)$, i.e.,

$$\hat{\xi}(k) \overset{k \to k_c}{\sim} \exp\left[\frac{\log l \, |\log(k_c - k)|^{1/2}}{(\log 5/2)^{1/2}}\right] \tag{3.25}$$

which, along with (2.14), yields

$$\langle R_N^2 \rangle^{1/2} \overset{N \gg 1}{\sim} \exp\left\{ \log l \left[\frac{\log N}{\log(5/2)} \right]^{1/2} \right\} \tag{3.26}$$

where l is the generic length scale. This is obviously slower than the usual power law [see Eq. (3.7)]. In this sense we shall say that the IC is localized!

We now turn to the determination of the entropic exponent γ. The recursion equations for the fields $h_x = h_2$, h_3 corresponding to $z_x = 2$, 3 are

$$h_2' = \left(\frac{\alpha_2^2 A}{2} \right)^{1/2} \left\{ h_2 \left[1 + \frac{2}{\alpha_2} + \frac{2}{\alpha_2^2 A} \left(2 + \alpha_3 - \frac{1}{\alpha_2} \right) \right] + h_3 \frac{2}{\alpha_2 A} \left(2 + \alpha_3 - \frac{1}{\alpha_2} \right) \right\} \tag{3.27a}$$

$$h_3' = \left(\frac{\alpha_2^2 A}{2} \right)^{1/2} \left\{ h_3 \left[1 + \frac{3}{\alpha_2 A} + \frac{3}{\alpha_2^2 A} \left(2 + \alpha_3 - \frac{1}{\alpha_2} \right) \right] + h_2 \left[\frac{3}{\alpha_2} + \frac{3}{\alpha_2^2 A} \left(2 + \alpha_3 - \frac{1}{\alpha_2} \right) \right] \right\} \tag{3.27b}$$

where $A = (\alpha_3 - 1/\alpha_2)^2 - 4$.

At the fixed point W, the highest eigenvalue of the linearized mapping (3.27a) and (3.27b) is $\lambda_h \equiv l^{y_h} = 9\sqrt{2}$, which defines y_h, for a general scaling factor l. The γ_w is given by (3.11) along with $d_w = \log 27/\log l$ and $\bar{d} = \log 6/\log l$; we find $\gamma_w = 1$, as expected.

The procedure for the other fixed point C is more complex and is sketched in Appendix B. The result is $\gamma_c = 1$.

The calculation of the return probability goes along the same lines as in the previous section. Being more complex, it is also outlined in Appendix B. We find $\tilde{d}_w/2 = \bar{d}/d_w = \log 6/\log 27$ and $\tilde{d}_c/2 = 0.5 < \tilde{d}_w/2$.

3.3. The Sierpinski Gasket

Another interesting model where the sites with highest connectivity do not form an infinite connected cluster is the Sierpinski gasket with generator 3×3 (Fig. 2).

The procedure is similar to that of the previous sections and we will not give annoying details. Here $z_x = 4$, 6. The recursions for the α's are

$$\alpha_4' = \frac{\alpha_4 - 4A}{C + B} \tag{3.28a}$$

$$\alpha_6' = \frac{\alpha_6 - 6A}{C + B} \tag{3.28b}$$

where

$$A = \frac{D}{\alpha_6(\alpha_4^2 - 1)} [\alpha_6\alpha_4(\alpha_4 - 1) - 4\alpha_4 - \alpha_6 - 2] \tag{3.29a}$$

$$B = \frac{2 + \alpha_6}{[(\alpha_4 - 2)\alpha_6 - 6](1 + \alpha_4)} \tag{3.29b}$$

$$C = \frac{4 + 2\alpha_4 + \alpha_6}{(\alpha_4^2 - 1)[(\alpha_4 - 2)\alpha_6 - 6]} \tag{3.29c}$$

$$D = \frac{\alpha_6}{(\alpha_4 - 2)\alpha_6 - 6} \tag{3.29d}$$

Again for the RW we have a fixed $W = (\alpha_4^* = 4, \alpha_6^* = 6)$ and an exponent $d_\omega = \log(90/7)/\log 3$. For the IC instead an analysis similar to that of the previous section yields $1/k_c = 0.371...$ and, after some tedious algebra,

$$\langle R_N^2 \rangle^{1/2} \sim (\log N)^{\log 3/\log 2} \tag{3.30}$$

The fixed point giving such a behavior is $C = (\alpha_4^* = +\infty, \alpha_6^* = 0)$. For the entropic exponent one finds $\gamma_w = 1$ and $\gamma_c = 3/2$.

In conclusion, on deterministic fractals, in the event that the sites of highest coordination do not form an infinite network, there is a localization effect (i.e., a diffusion in the presence of traps is slower than a power law) due to the entropic trapping. This is essentially due to a combined effect of self-similarity and nonuniform coordination. The fixed point in the RG recursions describing the IC is of a nonstandard type since it is infinitely repulsive, leading to a non-power-law dependence in the end-to-end distance. Nevertheless, there is a critical line L which is attracted by C, describing the critical behavior of a blind ant in the presence of imperfect traps residing around the fractal.

One may then ask what happens when we are in the presence of a true disordered system with statistical self-similarity such as the percolation cluster at the percolation threshold.

We will tackle the problem numerically using exact enumeration techniques in the next section.

4. STATISTICAL FRACTALS

There have been many investigations of the RW on a percolation cluster at criticality (see, e.g., ref. 26 and references therein). It is now accepted that the end-to-end distance $\langle R_N^2 \rangle$ behaves as in Eq. (3.7) with $d_w \in (2.7, 2.8)$. Recently, however,[8,9] a similar investigation was carried out for the IC on the same structure, using exact enumeration techniques.

Some of the results presented have appeared in refs. 8 and 9. Here we will discuss some new results and the details of the numerical technique. Because of the much improved statistics, some of the results given here supersede the estimates previously given.[8] All the numerical results presented in this section thus refer to the IC.

4.1. Exact Enumeration and Transfer Matrix

Let w_0 be a chain starting from $\mathbf{x}_0 \in \mathbb{Z}^d$. We are interested in the total number of chains originating from $\mathbf{x}_0$ ending everywhere, after N steps, and belonging to a cluster $\mathscr{C}$ of occupied sites, i.e.,

$$C_{\mathbf{x}_0}(N; \mathscr{C}) = \sum_{\mathbf{x}} C_{\mathbf{x}_0, \mathbf{x}}(N) = \sum_{w_0} \theta(w_0, \mathscr{C}) \tag{4.1}$$

where

$$\theta(w_0, \mathscr{C}) = \begin{cases} 1 & \text{if} \quad w_0 \subset \mathscr{C} \\ 0 & \text{otherwise} \end{cases} \tag{4.2}$$

The quenched average is defined as

$$\overline{C_{\mathbf{x}_0}(N)} = \sum_{\mathscr{C}} \mathscr{P}(\mathscr{C})\, C_{\mathbf{x}_0}(N; \mathscr{C}) \tag{4.3}$$

where $\mathscr{P}(\mathscr{C})$ is the probability of occurrence of a given configuration $\mathscr{C}$, which will be taken independent of $\mathscr{C}$ in what follows.

Similarly the (quenched) average end-to-end distance is

$$\overline{\langle R_N^2 \rangle} = \sum_{\mathscr{C}} \mathscr{P}(\mathscr{C}) \frac{\sum_{w_0} \theta(w_0, \mathscr{C})\, R_N^2(w_0)}{\sum_{w_0} \theta(w_0, \mathscr{C})} \tag{4.4}$$

where $R_N^2(w_0)$ is the end-to-end distance of the chain w_0.

The disordered lattice we will consider is the incipient infinite percolation cluster $\mathscr{C}$. On a square or cubic lattice a given site is open (or accessible) with probability p and closed (not available) with probability $1-p$. A cluster $\mathscr{C}$ is a subset of open sites: a site belongs to $\mathscr{C}$ if it is an open site nearest of a site of $\mathscr{C}$. Then it is well known that a critical threshold p_c exists above which at least an infinite cluster is present.[27] At $p = p_c$ the incipient infinite cluster (percolation cluster) is a statistical fractal.[28]

It is important to notice that random walks in the presence of traps independently distributed on each site with probability $1-p$, with p arbitrary and not necessarily equal to p_c, have been studied for a long time.[15,29,30] There the starting point is taken randomly on a finite or

infinite cluster $\mathscr{C}$. Here we work at $p = p_c$ and the starting point is taken on the infinite cluster. The sites not belonging to the infinite cluster act as a trapping environment.

The algorithm we will use to generate infinite incipient clusters is known as breadth-first search and it is standard.[6]

If $S(\mathscr{C})$ is the number of total sites present in a cluster $\mathscr{C}$, we can pass from the discrete time N to the discrete time $N+1$ for a given configuration $\mathscr{C}$ in Eq. (2.4) by applying on $S(\mathscr{C}) \times S(\mathscr{C})$ matrix $W_{\mathbf{x},\mathbf{y}}(\mathscr{C})$ such that

$$W_{\mathbf{x},\mathbf{y}}(\mathscr{C}) = \begin{cases} 1 & \text{if } |\mathbf{x}-\mathbf{y}| = 1; \quad \mathbf{x}, \mathbf{y} \in \mathscr{C} \\ 0 & \text{otherwise} \end{cases} \tag{4.5}$$

so that Eq. (2.4) can be rewritten in term of a transfer matrix formalism:

$$|\Psi(N)\rangle = W^N(\mathscr{C})\,|\Psi(0)\rangle \tag{4.6}$$

where $\langle \mathbf{x}|\,\Psi(N)\rangle \equiv C_{\mathbf{x}_0,\mathbf{x}}(N)$ is a column vector defining the state of the system at the discrete time N.

The total number of N-step chains with origin in $\mathbf{x}_0$ can then be obtained as a scalar product of the final state $|\Psi(N)\rangle$ and the state $|\Phi\rangle$ [whose dimension is $S(\mathscr{C})$] defined such that $\langle \mathbf{x}\,|\,\Phi\rangle = 1$ for all $\mathbf{x}$.

That is,

$$C_{\mathbf{x}_0}(N;\mathscr{C}) = \langle \Phi|\,\Psi(N)\rangle = \langle \Phi|\,W^N|\,\Psi(0)\rangle \tag{4.7}$$

where $\langle \mathbf{x}\,|\,\Psi(0)\rangle = \delta_{\mathbf{x}_0,\mathbf{x}}$ represents the initial state.

A similar procedure can be followed for the evaluation of the numerator of $\overline{\langle R_N^2\rangle}$ appearing in (4.4) with the substitution $\Phi \to \hat{\Phi}$ such that $\langle \mathbf{x}\,|\,\hat{\Phi}\rangle = |\mathbf{x}-\mathbf{x}_0|^2$.

Clearly a naive application of Eq. (4.7) would bring an overflow in the numerical computation after few steps since the number of walks is exponentially increasing. In order to avoid this we introduce normalized vectors u_j in the following way:

$$u_0 = \Psi(0), \qquad W|u_j\rangle = |u_{j+1}\rangle\, c(j), \qquad c(j) = \frac{\|\Psi(j+1)\|}{\|\Psi(j)\|} \tag{4.8}$$

Then Eq. (4.7) becomes

$$C_{\mathbf{x}_0}(N;\mathscr{C}) = \prod_{j=1}^{N} \|c(j)\|\,\langle \Phi|\,u_N\rangle \tag{4.9}$$

[6] For a general reference see, e.g., Kirkpatrick.[31]

or

$$\log C_{x_0}(N;\mathscr{C}) = \log\langle \Phi | u_N \rangle + \sum_{j=1}^{N} \log \| \Psi(j) \| \tag{4.10}$$

The overflow is thus avoided by working only with logarithms. The final result is exponentialized before taking the average over the disorder.

The algorithm for the calculation of the return probability discussed in the next section works in a similar way.

4.2. End-to-End Distance and Return Probability

Using the numerical method described in the previous section, we performed an extensive numerical analysis of $C_{x_0}(N;\mathscr{C})$ and $\overline{\langle R_N^2 \rangle}$ in two- and three-dimensional percolating clusters. Figure 4 shows, for the same configuration in $d=2$ and the same starting point, the comparison between RW and IC, making apparent the difference between the two types of diffusion. The behavior of the IC is not a smooth power law as in the case of the random walk (both blind and myopic ants)! Instead, an irregular curve with large plateaus followed by jumps is obtained. This is a peculiar result of the IC and it is an entropic effect similar to the one found for deterministic fractals studied in Section 3. The chain does not visit uniformly the

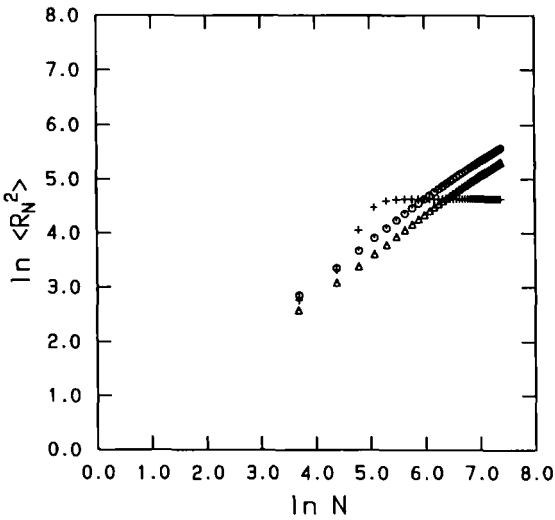

Fig. 4. Comparison on a log-log plot of the behavior of the myopic ant (○), blind and (△), and ideal chain (+) for the same fixed configuration in the case $d=2$.

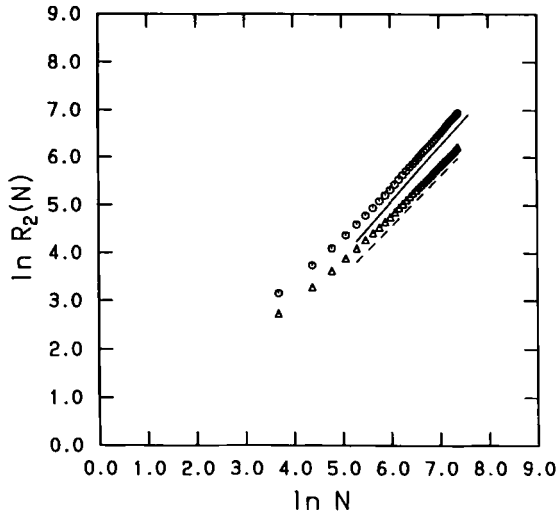

Fig. 5. A log-log plot for the end-to-end distance $R_2(N) \equiv \overline{\langle R_N^2 \rangle}$ for $d=2$ (○) and $d=3$ (△). The solid and dashed lines have slopes 1.16 and 1.04, respectively.

structure, but it tries to stay in regions with high connectivity. When the average over the disorder is taken, the usual power law (3.7) is recovered. The average is taken only on the infinite clusters and was carried out over six different sets of data, each of 1000 configurations.

In Fig. 5 we show $\overline{\langle R_N^2 \rangle}$ versus N, is a log–log plot, for both the two- and three-dimensional cases. Our best estimate of the exponents is $\nu_c = 0.58 \pm 0.03$ and $\nu_c = 0.52 \pm 0.03$ in $d=2$ and 3, respectively. These values reflect much improved statistics compared with our previous estimates in ref. 8. This is derived by averaging the exponents coming from best fit, Padé analysis, and standard extrapolating techniques. All exponents calculated in this section are summarized in Tables I and II. The same results are obtained if the quenched averages are taken by averaging

Table I. Summary of the Exponents ν, δ, and $\tilde{d}/2$, Obtained in the Text[a]

d	ν	δ	$\tilde{d}/2$
2	0.58 ± 0.03	1.60 ± 0.03	0.94 ± 0.06
3	0.52 ± 0.03	1.66 ± 0.03	1.05 ± 0.05

[a] The exponent ν refers to the average value of the three methods mentioned in the text, while both δ and $\tilde{d}/2$ were obtained by best fit.

Table II. Summary of the Exponents ψ and χ Defined in the Text[a]

d	ψ(D)	ψ(I)	χ(D)	χ(I)
2	0.80 ± 0.01	0.80 ± 0.01	0.68 ± 0.01	0.66 ± 0.01
3	0.85 ± 0.01	0.85 ± 0.02	0.75 ± 0.01	0.74 ± 0.01

[a] The labels (D) and (I) indicate direct evaluation and from the log-normal distribution, respectively.

over many different starting points $\mathbf{x}_0$ on a fixed configuration $\mathscr{C}$. This was expected since the same cluster looks different when seen from different points.

For the ants, i.e., RW, on the same structure it is already known that $\nu_w \sim 0.37$ and 0.28 in $d=2$ and 3, respectively. Thus it is remarkable that $\nu_c > \nu_w$ as we found in the exactly solvable model on the T-fractal. In other words, diffusion of the surviving ants in the presence of traps is faster (superdiffusion) than standard diffusion of the blind and myopic ants.

It is intriguing that in $d=2$, ν_c is greater than its counterpart in the translational-invariant lattice, where $\nu = 1/2$ (see Section 3).

Let us now investigate the scaling form of the distribution $P(\mathbf{R}, N)$ of the end-to-end distance $\mathbf{R} = \mathbf{x} - \mathbf{x}_0$. This is defined as [see also Eq. (3.16)]

$$\overline{P(\mathbf{R}, N)} = \sum_{\mathscr{C}} \mathscr{P}(\mathscr{C}) \frac{P_{\mathbf{x}_0,\mathbf{x}}(N, \mathscr{C})}{\sum_{\mathbf{x}} P_{\mathbf{x}_0,\mathbf{x}}(N, \mathscr{C})} \tag{4.11}$$

where $P_{\mathbf{x}_0,\mathbf{x}}(N, \mathscr{C}) = C_{\mathbf{x}_0,\mathbf{x}}(N, \mathscr{C})/z^N$ according to Eq. (2.6a) and it coincides with $\overline{P_{\mathbf{x}_0,\mathbf{x}}(N)}$ only for RW due to probability conservation, Eq. (2.21). The exact form of this function is still disputed in the random walk case, although there are heuristic arguments, supported by numerical simulations, predicting a stretched-exponential type of decay with an exponent $\delta = (1-\nu_c)^{-1}$.[19] This is the same scaling law which was shown by Fisher to hold in the case on the self-avoiding walk (with no disorder).[18]

If scale invariance holds, one expects that

$$\overline{P(\mathbf{R}, N)} = \frac{1}{N^{\bar{d}\nu_c}} F\left(\frac{R}{N^{\nu_c}}\right) \tag{4.12}$$

where $F(x)$ is a universal function such that $F(x) \sim \exp(-x^{\delta})$ for $x \gg 1$ and $F(x) \sim x^{\theta}$ for $x \to 0$. Since the support of the measure has a fractal of dimension $\bar{d}$, one has that

$$\int d^d R\, \rho(R)\, \overline{P(\mathbf{R}, N)} = S_d \int dx\, x^{\bar{d}} F(x) = 1 \tag{4.13}$$

where $\rho(R) = R^{\bar{d}-d}$ ($\bar{d} = 91/48 \sim 1.9$ and ~ 2.5 for $d = 2$ and 3, respectively[28]) and $S_d = 2\pi^{d/2}/\Gamma(d/2)$.

Figure 6 is a plot of $RP_N(R)/S_d = x^{\bar{d}}F(x)$ [$x = R/N^{\nu_c}$, where $P_N(R)$ is the probability obtained by $\overline{P(\mathbf{R}, N)}$ by separating off the angular part]. The data shown are for $d = 2$ and $N = 400$, 800, 1200, 1600. Within the statistical errors the collapse of the data is satisfactory for the value $\nu_c = 0.58$, thus supporting the above scaling form. A best fit gives $\delta = 1.60 \pm 0.11$ and $\delta = 1.67 \pm 0.03$ for $d = 2$ and 3, respectively. These values are not consistent with the scaling law $\delta = (1 - \nu_c)^{-1}$, which would give $\delta = 2.38 \pm 0.01$ and $\delta = 2.08 \pm 0.01$ for $d = 2$ and 3, respectively, using our aforementioned estimates for ν_c. We also find $\theta = -0.29 \pm 0.03$ and $\theta = -0.55 \pm 0.04$ for $d = 2$ and 3, respectively.

A value of δ which is consistent with our findings can be obtained by looking at the dimensionless moments:

$$m_q(N) = \frac{(\overline{\langle R_N^q \rangle})^{1/q}}{\langle R_N \rangle} = \Gamma^{1/q}\left(\frac{q + \bar{d} + \theta}{\delta}\right) \frac{\Gamma^{1 - 1/q}((\bar{d} + \theta)/\delta)}{\Gamma((1 + \bar{d} + \theta)/\delta)} \tag{4.14}$$

where the second equality has been obtained by assuming the form (4.12) with $F(x) \propto x^{\theta} \exp(-x^{\delta})$. By computing directly the higher moments

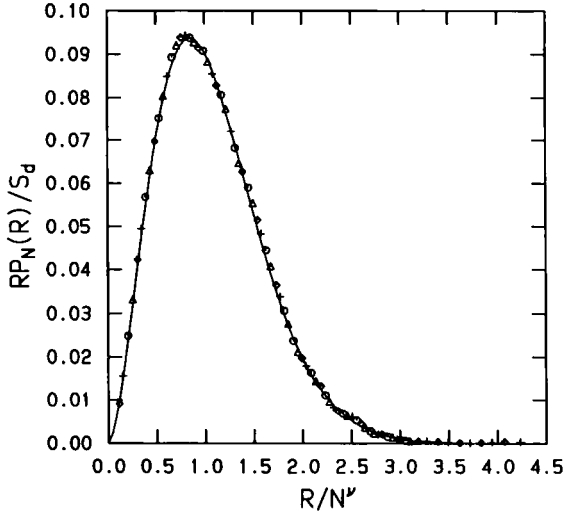

Fig. 6. Plot of the universal function $RP_N(R)/S_d = x^{\bar{d}}F(x)$ versus the dimensionless quantity R/N^{ν_c} for $d = 2$. We find $F(x) = Ax^{\theta}\exp(-Bx^{\delta})$. The data shown are for $N = 400$ ($\bigcirc$), $N = 800$ ($\triangle$), $N = 1200$ ($+$), $N = 1600$ ($\diamond$). The data shown are an average over five points. The solid line is the best fit result which gives $\delta = 1.60 \pm 0.03$ and $\theta = -0.29 \pm 0.03$. The collapsing of the data in a single curve supports the above scaling form. The value chosen for ν is 0.58.

($q = 0.5$, 1.5, 2) and comparing with Eq. (4.14), we find for $d = 2$ the best match for $\delta \sim 1.60$ and $\theta \sim -0.25$, in agreement with the previous estimate. The same type of agreement is also obtained for $d = 3$.

We have also considered a possible multifractal behavior for $m_q(N) \sim N^{\nu(q)-\nu(1)}$. With a satisfactory degree of accuracy we find $\nu(q) = \nu(1)$ for $q = 0.5$, 1.5, 2, in agreement with the prediction from the scaling form (4.12).

The return probability is defined, upon quenched average, as

$$\overline{P(\mathbf{0}, N)} = \sum_{\mathscr{C}} \mathscr{P}(\mathscr{C}) \frac{P_{\mathbf{x}_0, \mathbf{x}_0}(N, \mathscr{C})}{\sum_{\mathbf{x}} P_{\mathbf{x}_0, \mathbf{x}}(N, \mathscr{C})} \tag{4.15}$$

and is expected, according to Eq. (4.12), in the $R/N^{\nu} \to 0$ limit, to behave as

$$\overline{P(\mathbf{0}, N)} \overset{N \gg 1}{\sim} N^{-\tilde{d}_c/2} \tag{4.16}$$

with

$$\tilde{d}_c = 2(\tilde{d} + \theta)\, \nu_c \tag{4.17}$$

which can be regarded as a generalization of the usual Alexander–Orbach relation,[23] which is recovered for $\theta = 0$. It is worth noticing that this is the same situation as the T-fractal studied in Section 3.1, where the diffusion

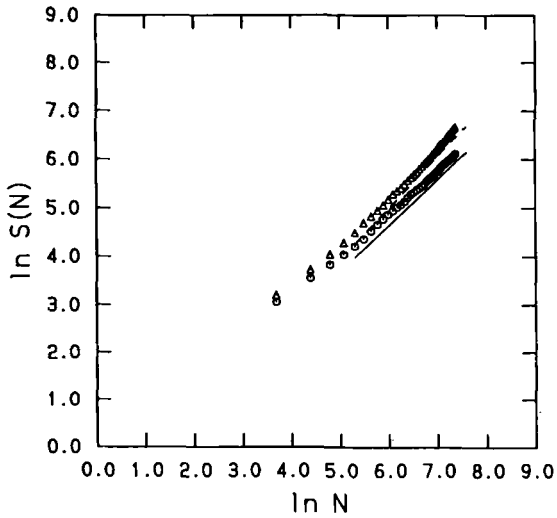

Fig. 7. A log-log plot of the quantity $S(N) \equiv \overline{P(\mathbf{0}, N)}^{-1} \sim N^{\tilde{d}/2}$ for $d = 2$ (○) and $d = 2$ (△). The solid and dashed lines have slopes 0.94 and 1.05 for $d = 2$ and $d = 3$, respectively.

was also faster for the IC than for the RW. We recall that $\tilde{d}$ is an intrinsic quantity, in contrast to $\bar{d}$, θ, and $d_c = 1/\nu_c$, in the sense that it is independent of the embedding space. It depends only on the topology $\mathscr{C}$, i.e., the assignment of the neighbors of any site of $\mathscr{C}$.[32] The values obtained by a direct computation are $\tilde{d}_c/2 = 0.94 \pm 0.06$ for $d = 2$ and $\tilde{d}_c/2 = 1.05 \pm 0.05$ for $d = 3$, consistent with Eq. (4.17) and previously computed values, which would give $(\bar{d} + \theta)\nu_c = 0.94 \pm 002$ and 1.02 ± 0.03 for $d = 2, 3$, respectively (see Fig. 7). This has also an interesting physical interpretation. It is well known[3,4] that for the self-avoiding walk (and no disorder), $\theta = (\gamma - 1)/\nu$. The fact that $\theta > 0$ means that it is difficult for a walk to return to the origin. For the ideal chain instead $\theta < 0$ and the return is more likely, which is consistent with the entropic trapping occurring for the single realization as discussed at the beginning of this subsection. For the random walk, on the other hand, $\theta = 0$[23] and the return is unbiased.

4.3. Distribution of the Number of Chains

We now turn to the interesting analysis of the entropic behavior. As mentioned in Section 4.1, the *tadpole* configuration assumed by the head of the chain is essentially an entropic effect due to the disorder. It is then natural to study the distribution of the number of chains, which in the absence of disorder would be a delta function centered in z^N (z is the coordination number of the lattice). On the basis that $C \equiv C_{x_0}(N, \mathscr{C})$ comes

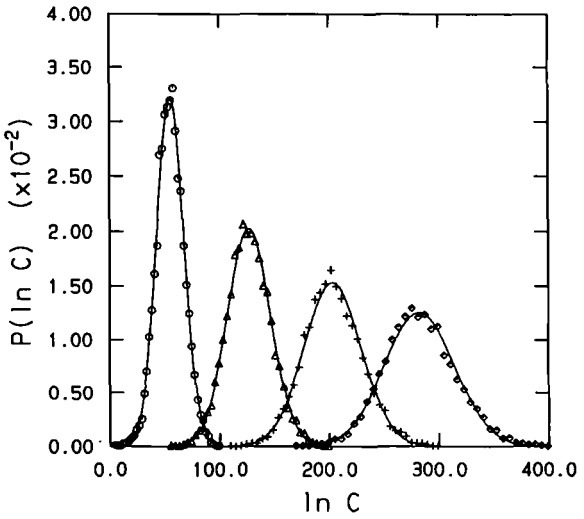

Fig. 8. Calculated distribution $P(\log C)$ for $N = 400$ (○), $N = 800$ (◇), $B = 1200$ (+), $N = 1600$ (◇), in the case $d = 2$. The solid lines are the best fit results derived from Eq. (4.18).

from a product of random matrices, one might expect the distribution to be log-normal. The numerical evaluation is shown in Fig. 8 for $N=400$, 800, 1200, 1600 in the case $d=2$, and it appears to be consistent with the prediction

$$P(C, N)=\frac{1}{C(2\pi\sigma_N^2)^{1/2}}\exp\left[-\frac{(\log C-\lambda_N)^2}{2\sigma_N^2}\right] \tag{4.18}$$

where the mean $\lambda_N=\overline{\log C_{x_0}(N, \mathscr{C})}$ and the variance $\sigma_N^2=\overline{(\log C_{x_0}(N, \mathscr{C}))^2}-(\overline{\log C_{x_0}(N, \mathscr{C})})^2$ both depend on N. The solid line represents the best fit. Consistently, we can plot the results for different N in terms of the scaled variables $\Delta y=(\log C-\lambda_N)/(2\sigma_N^2)^{1/2}$ and of the function $p(\Delta y)=(2\pi\sigma_N^2)^{1/2}P(\log C)$, where $P(\log C)=CP(C, N)$. The collapsing of the data to a single universal curve is rather good (see Fig. 9), thus supporting the above log-normal form.

In the large-N limit the mean scales like $\lambda_N=N\log\mu-\alpha N^{\psi}$, with $\psi(I)=0.80\pm0.01$ and 0.85 ± 0.02 for $d=2, 3$, respectively. Instead for the variance we find a best fit of the form $\sigma_N^2\cong N^{2\chi}$ with $\chi(I)=0.66\pm0.01$ and 0.74 ± 0.01 for $d=2, 3$, respectively. The index I indicates that the exponents have been derived from the shape of the log-normal distribution, to be distinguished from the case when a more direct evaluation (i.e., from the moments) is performed.

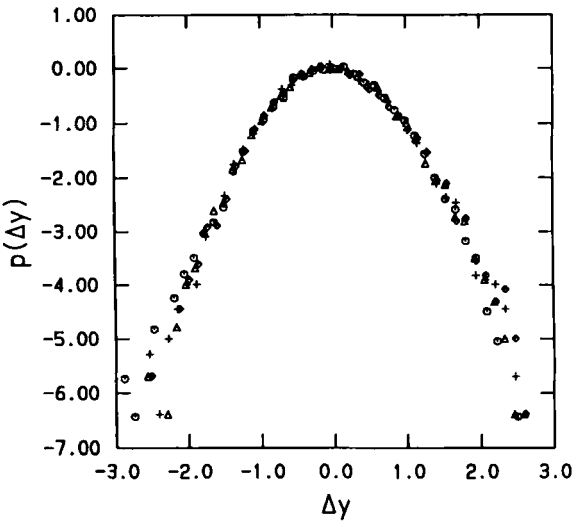

Fig. 9. Plot of the distribution $p(\Delta y)=P(\log C)(2\pi\sigma_N^2)^{1/2}$ in terms of the scaled variable $\Delta y=(\log C-\lambda_N)/(2\sigma_N^2)^{1/2}$. The values are $N=400$ (○), $N=800$ (△), $N=1200$ (+), $N=1600$ (◇).

The extremely important feature to be noticed is that $\sigma_N^2 \gg \lambda_N$ (for large N), which would not happen in the absence of disorder as a central limit theorem. This does not create particular problems for the logarithmic moments like

$$L_q(N) \equiv \overline{(\log C_{\mathbf{x}_0}(N, \mathscr{C}))^q}^{1/q} \tag{4.19}$$

In particular, then, $L_0(N) = \lambda_N$, whose direct numerical evaluation gives a value which is in perfect agreement with the above assumption, namely $\psi(D) = 0.80 \pm 0.01$ and 0.85 ± 0.01, for $d = 2, 3$, respectively. The other parameters were found compatible as well. Indeed (for $d = 2$) we found $\mu = 3.76 \pm 0.01$ and $\alpha = 0.52 \pm 0.01$ from the log-normal distribution and $\mu = 3.76 \pm 0.02$ and $\alpha = 0.52 \pm 0.01$ directly. Similar agreement holds for $d = 3$. Furthermore, a direct evaluation of σ_N^2 gives $\chi(D) = 0.68 \pm 0.01$ and 0.75 ± 0.01 in the cases $d = 2, 3$, respectively.

We also computed the fourth and sixth cumulants for the distribution $P(\log C)$ and found them to vanish, as they should for a Gaussian distribution.

Note that this behavior for the logarithmic moment is of the type defined in Eq. (2.26), which predicts an essential singularity for the susceptibility [Eq. (2.27)] upon exponentiation.

However, a log-normal distribution would give for the moments $Z_q(N) \equiv \overline{C_{\mathbf{x}_0}^q(N, \mathscr{C})}^{1/q}$ a behavior

$$Z_q(N) = \exp(\lambda_N + \tfrac{1}{2}\sigma_N^2 q) \tag{4.20}$$

In view of the fact that $\sigma_N^2 \gg \lambda_N$ for large N this is inconsistent with the bounds $1 \leqslant Z_q(N) \leqslant z^N$. When $\sigma_N \ll \lambda_N \ll \sigma_N^2$ we will speak of *weak lack of self-averaging* to be distinguished from the standard lack of self-averaging.[33]

The source of the problem for the log-normal distribution is well known to come from the tail of the distribution itself, which fails to drop to zero sufficiently fast. As a consequence the knowledge of all the moments does not define the distribution univocally.[34]

This apparent paradox is solved by assuming a cutoff $\sim z^N$ in the distribution, i.e.,

$$\overline{C_{\mathbf{x}_0}^q(N, \mathscr{C})} = \int_1^{z^N} dC\, C^q P(C, N) \Big/ \int_1^{z^N} dC\, P(C, N) \tag{4.21}$$

It is easily seen that this has no effect on the asymptotic behavior of the logarithmic moments in Eq. (4.19).

In order to perform the integral, it is useful to introduce an auxiliary variable through an Hubbard–Stratonovitch type of transformation:

$$\exp\left(-\frac{1}{2}\frac{y^2}{\sigma_N^2}\right)=\left(\frac{\sigma_N^2}{2\pi}\right)^{1/2}\int_{-\infty}^{+\infty} d\alpha \exp\left(-\frac{1}{2}\sigma_N^2\alpha^2+i\alpha y\right) \tag{4.22}$$

The result is, dropping subdominant terms,

$$\overline{C_{x_0}(N,\mathscr{C})^q}=\exp(\lambda_N q+q^2\sigma_N^2/2)\,Q(\sigma_N[q-\hat{\lambda}_N/\sigma_N^2]) \tag{4.23}$$

where $\hat{\lambda}_N = N\log z - \lambda_N$ and where we introduced the error function

$$Q(x)=\frac{1}{(2\pi)^{1/2}}\int_x^{+\infty} d\eta \exp\left(-\frac{1}{2}\eta^2\right) \tag{4.24}$$

Using the asymptotic expansion for the above error function, we then get the final result:

$$Z_q(N)=z^N \exp\left\{-\frac{1}{2q}\left[\log\left(\frac{z}{\mu}\right)\right]^2\frac{N^2}{\sigma_N^2}-\frac{\alpha}{q}\log\left(\frac{z}{\mu}\right)\frac{N^{1+\psi}}{\sigma_N^2}+O(N^{2(\psi-\chi)})\right\} \tag{4.25}$$

A numerical check of this behavior was found to be extremely hard to implement. The basic reason for this comes again from the lack of self-averaging. In order words, the fluctuations for the values of $C_{x_0}(N,\mathscr{C})$ are larger than the mean values. As a result the average over values of the variable $C_{x_0}(N,\mathscr{C})$ fails to include events which are far from the most probable one, which is represented by the logarithmic moment.

This possibility is well known to occur rather frequently in presence of disorder.[35]

It is interesting to notice that, if we identify z appearing in Eq. (4.21) with the coordination number of the lattice, then a scaling law similar to (4.25) has been proposed[15] for the survival probability, $P_S(N)=\overline{C_{x_0}(N,\mathscr{C})/z^N}$ of the IC when sites are open with probability p and closed with probability $1-p$. In d dimensions it was found that asymptotically[10,15,30]

$$P_S(N)\sim\exp[-|\log p^{2/(d+2)}N^{d/(d+2)}] \tag{4.26}$$

However, at variance with our case, where the chain is contained in the infinite cluster at the percolation threshold p_c, here the chain can live on finite clusters of occupied sites (in fact it is the only possibility when $p<p_c$).

The possibility of scaling behavior like (4.26) at $p < p_c$ is characteristic of this problem of random paths where no excluded-volume effect is present. For ordiniary spin systems in a diluted lattice with short-range interaction or self-avoiding walks, no critical behavior can be observed below p_c.

If we restrict the average on the infinite clusters, then, to the best of our knowledge, there are no rigorous results of the type (4.26). An extension of the heuristic argument similar to the one presented in refs. 30 and 5 would lead to the result

$$P_S(N) \sim \exp[-AN^{\tilde{d}\nu_c/(\tilde{d}\nu_c+1)}] \tag{4.27}$$

where A is a constant. Note that, according to the results of Section 4.2, the exponent is different from the one obtained from the substitution $d \to \tilde{d}$.

Comparison of Eq. (4.25) with Eq. (4.27) yields

$$\chi = \frac{\tilde{d}\nu_c + 2}{2\tilde{d}\nu_c + 2} \tag{4.28}$$

This conjecture would give, using our values for ν_c, $\chi = 0.74 \pm 0.02$ and 0.72 ± 0.01 for $d = 2, 3$, respectively. Although these values are very close to our finding, particularly for the three-dimensional case, the dependence on the dimensionality does not seen to be correct. This should not be surprisingly, however: besides the constraint of the fractal environment, it appears that the above argument cannot catch the essential feature of the strongly correlated disorder related to the choice of averaging only on the incipient infinite cluster.

As in the case of the deterministic fractals it is interesting to ask what is the universality class of the intermediate case described by Eq. (2.16) with $q \in (0, 1)$ (the imperfect blind ant). We checked that as soon as $q < 1$ the universality class is the one of the ideal chain. It is also possible to derive a simple argument relating the number of steps necessary to exit from the transient region with the value of q.

5. CONCLUSIONS

In this paper we presented an investigation of the problem of static random paths (ideal chain) both on deterministic and statistical fractals using analytical (renormalization group) and numerical (transfer matrix) techniques. On one hand, this model could be useful in the description of optical and/or magnetic excitations in the presence of fixed centers where the excitations decay (e.g., by fluorescence). On the other hand, the motion of single polymers in porous media can also be described in this way.

Due to the equivalence between kinetic and static random paths (i.e., random walks) on translationally invariant (e.g., hypercubic) lattices, this equivalence was tacitly assumed to hold in any environment. We find instead that the universality class of this model is different on non-translationally-invariant lattices such as self-similar structures.

This model is also an interesting limiting case of the self-avoiding walk on strongly correlated disordered structures, when the self-avoidcance is negligible.

On the methodological standpoint, the RG analysis done here in the case of the ideal chain is nonstandard due to the appearance of singularities in the recursion relations associated to a new types of fixed points.[7] We have also found that the ideal chain shows unexpected novel behavior both in the deterministic and in statistical fractals.

In particular, the end-to-end distance behavior ranges from very slow (e.g., logarithmic) diffusion to superdiffusion. The entropic behavior also appears to be different in the presence of disorder, depending on whether the average (first moment) or the most probable (logarithmic moment) is considered for the number of chains. The distribution of the number of N-step chains is log-normal with a variance growing with N faster than the average, leading to a non-self-averaging behavior.

It would be extremely interesting to carry out a similar investigation in the presence of self-avoidance, whose critical properties are still not fully understood.

APPENDIX A. GENERAL PROCEDURE FOR SINGULAR RECURSIONS

Let us consider the 2D map

$$\begin{aligned} x' &= R_x(x, y) \\ y' &= R_y(x, y) \end{aligned} \tag{A1}$$

For simplicity we assume that this has a fixed point at $O = \{x^* = 0, y^* = 0\}$ in the sense that either it satisfies identically (A1) or is a singular point but there is a (critical) invariant line L which is attracted by it. In the latter case the standard procedure of linearizing around it to extract asymptotic behaviors does not work. We now want to describe an alternative procedure and show that this is equivalent to the usual case in the event that the linearization is possible.

[7] Recently the same type of singularity has been found to occur for diffusion in ramified structures in the presence of an external bias.[136]

Let $L: y = y(x)$ be such that

$$\begin{aligned} &\text{(i)} && y(x) \xrightarrow{x \to x^*} y^* \\ &\text{(ii)} && x' = R_x(x, y(x)) \\ &\text{(iii)} && y' = R_y(x, y(x)) = y(x') \end{aligned} \tag{A2}$$

The condition (iii) simply means that the line L is invariant under the recursions (A1).

Let us start from a point $\bar{P} = (\bar{x}, y(\bar{x}) + \delta)$, with $\delta \ll 1$, which is slightly above the critical line $y = y(x)$. Under the recursions (A1), the point is driven into $\bar{P}' = (\bar{x}', y(\bar{x}') + \delta')$. We then can easily find the relation between δ' and δ, i.e., how the point is driven away from the critical line, due to the repulsive eigenvalue. At the leading order

$$\bar{y}' \equiv R_y(\bar{x}, y(\bar{x}) + \delta) = R_y(\bar{x}, y(\bar{x})) + \frac{\partial}{\partial y} R_y(\bar{x}, y)\bigg|_{y = y(\bar{x})} \delta \tag{A3}$$

and

$$\begin{aligned} y(\bar{x}') &= y(R_x(\bar{x}, y(\bar{x}) + \delta)) \\ &= y[R_x(\bar{x}, y(\bar{x}))] + \frac{d}{dx} y(x)\bigg|_{x = R_x(\bar{x}, y(\bar{x}))} \frac{\partial}{\partial y} R_x(\bar{x}, y)\bigg|_{y = y(\bar{x})} \delta \end{aligned} \tag{A4}$$

Therefore, since $\delta' = \bar{y}' - y(\bar{x}')$, using condition (ii) of Eq. (A2), we find

$$\delta' = \Lambda \delta + O(\delta^2) \tag{A5}$$

where

$$\Lambda = \left[\frac{\partial}{\partial y} R_y(\bar{x}, y)\bigg|_{y = y(\bar{x})} - \frac{d}{dx} y(x)\bigg|_{x = R_x(\bar{x}, y(\bar{x}))} \frac{\partial}{\partial y} R_x(\bar{x}, y)_{y = y(\bar{x})} \right] \tag{A6}$$

We want to show that this coincides with the maximum eigenvalue in the standard case where its value is finite.

The scaling fields for this problem are

$$\begin{aligned} u_M(x, y) &= a_x x + a_y y + o(x^2, y^2, xy) \\ u_m(x, y) &= b_x x + b_y y + o(x^2, y^2, xy) \end{aligned} \tag{A7}$$

where u_M, u_m correspond to the maximum and minimum eigenvalues λ_M, λ_m, respectively. If M is the linearizing matrix of the recursions (A1)

around the fixed point (i.e., $M_{xx}=\partial x'/\partial x$, $M_{x,y}=\partial x'/\partial y$, etc.), then it is clear that a_x and a_y (b_x and b_y) are the components of the left eigenvector corresponding to $\lambda_M(\lambda_m)$. This thus gives for the maximum eigenvalue

$$\frac{a_x}{a_y}=\frac{M_{yx}}{\lambda_M-M_{xx}} \tag{A8}$$

The critical line can be found by imposing $u_M(x, y)=0$ which at the leading order gives

$$y(x)=-\frac{a_x}{a_y}x \tag{A9}$$

Thus, evaluation of the terms present in (A6) lead to

$$\Lambda=M_{yy}+\frac{M_{yx}M_{xy}}{(\lambda_M-M_{xx})} \tag{A10}$$

which coincides with λ_M, as is easy to verify.

APPENDIX B. CALCULATION OF THE EXPONENTS γ AND $\tilde{D}$ FOR THE BLOB-LINK MODEL

In this appendix we first describe the procedure to obtain the entropic exponent for the blob-link model starting from the recursions (3.27a) and (3.27b). It is convenient to redefine the fields as $b_r=h_r/\sqrt{\alpha_r}$ ($r=2, 3$). If we assume that we are on the critical line L, and thus use the leading orders in Eqs. (3.19) and (3.20) in Eqs. (3.27a) and (3.27b), then we have for the redefined fields b, after n iterations,

$$\begin{aligned} b_2^{(n)}&=A^n\lambda_1^{n^2/2}b_3 \\ b_3^{(n)}&=B^n\lambda_1^{n^2/2}b_3 \end{aligned} \tag{B1}$$

where A, B are constants and λ_1 was defined before as $\lambda_1=5/2$.

The scaling of the singular part of the free energy per site of the Gaussian model (2.7) after n iterations is

$$f(\alpha_2, \alpha_3, b_2, b_3)=l^{-n\bar{d}}f(\alpha_2^{(n)}, \alpha_3^{(n)}, b_2^{(n)}, b_3^{(n)}) \tag{B2}$$

Since the susceptibility χ is given by $\partial^2 f(\alpha_2, \alpha_3, b, b)/\partial b^2$, from (B2), (3.27a) and (3.27b) one derives that

$$\chi(\delta, \alpha_2)\overset{\delta\to 0}{\sim}\delta^{-1}+\text{subleading terms} \tag{B3}$$

from which $\gamma_c=1$, since $\delta=k_c-k$.

We now consider the calculation of the return probability. The renormalization of the two-point correlation function gives

$$G_{\mathbf{x}_0,\mathbf{x}_0}(\alpha_2, \alpha_3) = D(\alpha_2, \alpha_3)\, G_{\mathbf{x}_0,\mathbf{x}_0}(\alpha_2', \alpha_3') \tag{B4}$$

where

$$D(\alpha_2, \alpha_3) = \tfrac{1}{2}[(\alpha_2\alpha_3 - 1)^2 - 4\alpha_2^2] \tag{B5}$$

follows from the rescaling of the field [see Eq. (3.2)].

At the fixed point W this gives (for the random walk) $\tilde{d}_w/2 = \log 6/\log 27$, as expected.

For the other fixed point, we need to use Eqs. (3.19) and (3.20). Upon iteration and making use of Eq. (3.22), we get, using (B4) close to the critical line,

$$\tilde{G}(k) \overset{k \to k_c}{\sim} (k_c - k)^{-1/2} \tag{B6}$$

This, at the leading order, yields

$$P(\mathbf{0}, N) \sim N^{-\tilde{d}_c/2} \tag{B7}$$

with $\tilde{d}_c/2 = 1/2$ since $\gamma_c = 1$.

APPENDIX C. PERIODIC LATTICE WITH NONUNIFORM COORDINATION NUMBER

Here we want to show in a simple example that the nonuniform coordination number does not lead to new physics in a periodic lattice. The basic idea is based on the following. In the notations of Section 2 we consider the Fourier transform of the $P_{\mathbf{x}_0,\mathbf{x}}(N)$, namely

$$\tilde{P}(\mathbf{q}, N) = \sum_{\mathbf{x}} e^{-i\mathbf{q}\cdot(\mathbf{x}-\mathbf{x}_0)} P_{\mathbf{x}_0,\mathbf{x}}(N) \tag{C1}$$

Similarly, let $\tilde{G}(\mathbf{q}, \omega)$ be the Fourier transform of the generating function (2.2). Then it is easy to see that the end-to-end distance

$$\langle R_N^2 \rangle = -\nabla_{\mathbf{q}}^2 \tilde{P}(\mathbf{q}, N)|_{\mathbf{q}=0} \tag{C2}$$

has as a generating function:

$$-\nabla_{\mathbf{q}}^2 \tilde{G}(\mathbf{q}, \omega)|_{\mathbf{q}=0} = \sum_{N=0}^{+\infty} \frac{1}{z(1+\omega)^{N+1}} \langle R_N^2 \rangle \sim \omega^{-(2\nu_w+1)} \tag{C3}$$

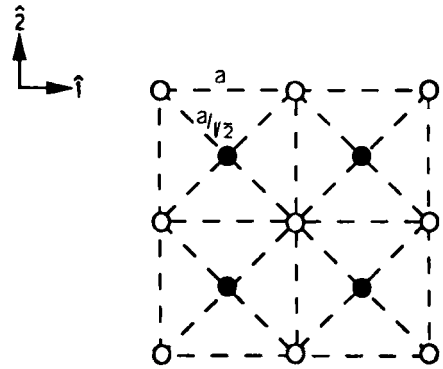

Fig. 10. Example of the lattice with basis considered in Appendix C. The sites $\mathbf{x} \in E_1 \equiv \{\bigcirc\}$ have coordination numbers $z_{\mathbf{x}} = 8$, while the sites $\mathbf{x} \in \{\bullet\}$ have coordination numbers $z_{\mathbf{x}} = 4$.

for $\omega \to 0$. This means that if the propagator $\tilde{G}(\mathbf{q}, \omega)$ in the continuous limit $a \to 0$ has the form

$$\tilde{G}(\mathbf{q}, \omega) \sim \frac{1}{A\omega + B\mathbf{q}^2} \tag{C4}$$

with A, B constants (depending on the lattice), then from (C3) we get $\nu_w = 1/2$, i.e., normal diffusion.

A simple two-dimensional example is depicted in Fig. 10. We add one more index α to the probability $P^{\alpha_0,\alpha}_{\mathbf{x}_0,\mathbf{x}}(N)$ such that $\mathbf{x}$ belongs to $E_1 \equiv \{\bigcirc\}$ and $\alpha = 0$ if the ant is at $\mathbf{x}$, whereas $\alpha = 1$ if the ant is at the center of the square whose lower left corner is $\mathbf{x}$. We allow jumps between sites at distance a and $a/\sqrt{2}$; then we have two different coordinations, namely $z_{\mathbf{x}} = 8, 4$. The solution of the master equation (2.1) is readily obtained by Fourier serie, (C1) where $\tilde{G}^{\alpha_0,\alpha}(\mathbf{q}, \omega)$ is now a 2×2 system. Then it is easy to see that equations of the form (C4) are found for $\tilde{G}^{\alpha_0,\alpha}(\mathbf{q}, \omega)\ \forall \alpha_0, \alpha$, thus leading to normal diffusion for both ants.

For the ideal chain, whose critical fugacity is not known *a priori*, it is also easy to see that the critical value k_c which makes the propagator massless is $k_c = (\sqrt{5} - 1)/8$, which belongs to the interval $[1/8, 1/4]$ as expected and again $\nu_c = 1/2$.

ACKNOWLEDGMENTS

A.G. wishes to thank the Department of Physics at the University of Padova for kind hospitality and INFN sez di Padova for partial financial support. The work of A.M. was partially supported by the U.S. Office of Naval Research.

REFERENCES

1. E. Montroll and G. Weiss, *J. Math. Phys.* **6**:167 (1965); M. Barber and B. Ninham, *Random and Restricted Walks. Theory and Applications* (Gordon and Breach, New York, 1970); C. Irzykson and J. M. Drouffe, *Statistical Field Theory*, Vol. 1 (Cambridge University Press, Cambridge, 1989).
2. K. Symanzik, in *Rendiconti della Scuola Internationale di Fisica "Enrico Fermi"* (Academic Press, New York, 1969); J. Frohlich, *Nucl. Phys. B* **200**[FS4]:281 (1982).
3. P. G. de Gennes, *Scaling Concepts in Polymer Physics* (Cornell University Press. Ithaca, New York, 1979).
4. J. des Cloizeaux and G. Jannik, *Polymers in Solution: Their Modelling and Structure* (Oxford University Press, Oxford, 1990).
5. J. W. Haus and K. W. Kehr, *Phys. Rep.* **150**:263 (1987).
6. P. de Gennes, *Recherche* 7:919 (1976); C. Mitescu and J. Roussenq, in *Percolation Structures and Processes*, G. Deutscher, R. Zallen, and J. Adler, eds. (Hilger, Bristol, 1983), p. 81.
7. A. Maritan, *Phys. Rev. Lett.* **62**:2845 (1989).
8. A. Giacometti, H. Nakanishi, A. Maritan, and N. H. Fuchs, *J. Phys. A: Math. Gen.* **25**:L461 (1992).
9. A. Giacometti and A. Maritan, *Phys. Rev. E* **49**:227 (1994).
10. I. Webman, *Phys. Rev. Lett.* **52**:220 (1984); P. Argyreakis and R. Kopelman, *Chem. Phys.* **78**:251 (1983).
11. P. Le Doussal and J. Machta, *J. Stat. Phys.* **64**:541 (1991), and references therein.
12. A. Maritan, *J. Phys. A* **21**:859 (1988); see also A. B. Harris, Y. Meir, and A. Aharony, *Phys. Rev. B* **38**:8752 (1987).
13. N. H. Fuchs and H. Nakanishi, *Phys. Rev. A* **43** (1991); H. Nakanishi, S. Mukherjee, and N. Fuchs, *Phys. Rev. E* **47**:R1463 (1993).
14. A. Giacometti and H. Nakanishi, submitted to *Phys. Rev. E* (1994).
15. M. Donsker and S. R. S. Varadhan, *Commun. Pure Appl. Math.* **28**:525 (1975); T. C. Lubensky, *Phys. Rev. A* **30**:2657 (1984); S. R. Renn, *Nucl. Phys. B* **275**[FS17]:273 (1986); Th. M. Nieuwenhuizen, *Phys. Rev. Lett.* **62**:357 (1989).
16. L. Balents and M. Kardar, *J. Stat. Phys.* **67**:1 (1992).
17. J. Feder, *Fractals* (Plenum Press, New York, 1988).
18. M. E. Fisher, *J. Chem. Phys.* **44**:616 (1966); see also P. Pincus, *Macromolecules* **9**:383 (1976).
19. A. Harris and A. Aharony, *Europhys. Lett.*. **4**:1355 (1987); A. Bunde, S. Havlin, and H. E. Roman, *Phys. Rev. A* **42**:6274 (1990).
20. G. H. Hardy, *Divergent Series* (Oxford University Press, Oxford, 1949).
21. J. Vannimenus and M. Knezevic, *Europhys. Lett.* **3**:21 (1987).
22. Th. Nieimejer and J. M. J. Leeween, *Phys. Rev. Lett.* **31**:1411 (1973).
23. S. Alexander and R. Orbach, *J. Phys.* (Paris) **45**:625 (1982).
24. A. Maritan, A. L. Stella, and F. Toigo, *Phys. Rev. B* **40**:9269 (1989).
25. L. de Arcangelis, S. Redner, and A. Coniglio, *Phys. Rev. B* **31**:4725 (1985).
26. D. Jacobs and H. Nakanishi, *Phys. Rev. A* **41**:706 (1990).
27. M. F. Sykes and J. W. Essam, *J. Math. Phys.* **5**:1117 (1964).
28. A. Coniglio, in *Magnetic Phase Transitions*, M. Ausloos and R. J. Elliot, eds. (Springer-Verlag, Berlin, 1983).
29. B. Ya. Balagurov and V. G. Vaks, *Sov. Phys.-JETP* **38**:968 (1974).
30. P. Grassberger and I. Procaccia, *J. Chem. Phys.* **77**:12 (1982).

31. S. Kirkpatrick, in *Ill-Condendensed Matter: Les Houches 1978*, R. Balian, R. Maynard, and G. Toulouse, eds. (North-Holland, Amsterdam, 1979).
32. R. Rammal and G. Toulouse, *J. Phys.* (Paris) **44**:L13 (1983).
33. K. Binder and A. P. Young, *Rev. Mod. Phys.* **58**:801 (1986).
34. S. A. Orszag, *Phys. Fluids* **13**:2211 (1970); see also W. Feller, *An Introduction to Probability Theory and Its Applications*, Vol. II, 2nd ed. (Wiley, New York, 1957).
35. B. Derrida, *Phys. Rep.* **103**:41 (1984).
36. A. Maritan, G. Sartoni, and A. I. Stella, *Phys. Rev. Lett.* **71**:1027 (1993).